FERMILAB-Pub-00/138-T
FTUAM 99-27
IFT-UAM 00-20
SCIPP 00/22
hep–ph/0007006
July 2000

SUSY-QCD corrections to the MSSM $h^0 b\bar{b}$ vertex in the decoupling limit

Howard E. Haber[a], María J. Herrero[b], Heather E. Logan[c], Siannah Peñaranda[b], Stefano Rigolin[d] and David Temes[b] *

[a] *Santa Cruz Institute for Particle Physics*
University of California, Santa Cruz, CA 95064, USA.
[b] *Departamento de Física Teórica*
Universidad Autónoma de Madrid, Cantoblanco, 28049 Madrid, Spain.
[c] *Theoretical Physics Department*
Fermi National Accelerator Laboratory, Batavia, IL 60510-0500, USA.
[d] *Department of Physics*
University of Michigan, Ann Arbor, MI 48109, USA.

Abstract

We analyze the supersymmetric (SUSY) QCD contribution to the $h^0 b\bar{b}$ coupling at one loop in the Minimal Supersymmetric Model (MSSM) in the decoupling limit. Analytic expressions in the large SUSY mass region are derived and the decoupling behavior of the corrections is examined in various limiting cases, where some or all of the SUSY mass parameters become large. We show that in the decoupling limit of large SUSY mass parameters and large CP-odd Higgs mass, the $h^0 b\bar{b}$ coupling approaches its Standard Model value at one loop. However, the onset of decoupling is delayed when $\tan\beta$ is large. In addition, the one-loop SUSY-QCD corrections decouple if the masses of either the bottom squarks or the gluino are separately taken large; although the approach to decoupling is significantly slower in the latter case.

*electronic addresses: haber@scipp.ucsc.edu, herrero@delta.ft.uam.es, logan@fnal.gov, siannah@delta.ft.uam.es, srigolin@umich.edu, temes@delta.ft.uam.es

1 Introduction

Once a light CP-even Higgs boson is discovered, it will be crucial to measure as many of its couplings as possible with the highest accuracy possible. By measuring the Higgs couplings to gauge bosons, one can learn whether only one Higgs boson is involved in electroweak symmetry breaking dynamics. Moreover, the Higgs couplings to vector bosons are sensitive to the possible existence of non-doublet isospin structure in the Higgs sector. By measuring the Higgs couplings to fermion pairs, one can learn whether the Higgs boson is responsible for fermion mass generation. Knowledge of the trilinear and quartic Higgs self-couplings, although extremely difficult to obtain, would allow one to reconstruct the Higgs potential and directly test the mechanism of electroweak symmetry breaking. Finally, if the couplings can be measured at the level of the radiative corrections, one could then derive significant constraints on new physics beyond the reach of the present accelerators. A detailed study of radiative corrections to the Higgs couplings would be especially important if a light Higgs boson were discovered in the mass range predicted by the minimal supersymmetric extension of the Standard Model (MSSM), but supersymmetric (SUSY) particles were not found. In this case, the precise experimental determination of Higgs couplings could provide indirect information about the preferred region of SUSY parameter space. For example, one could predict (in the context of the MSSM) whether the data favored a SUSY spectrum below the 1 TeV energy scale.

It is well known that the tree-level couplings of the lightest MSSM Higgs boson (h^0) to fermion pairs and gauge bosons tend to their Standard Model (SM) values in the decoupling limit, $M_A \gg M_Z$ [1], where M_A is the mass of the CP-odd neutral Higgs boson (A^0) of the MSSM. As a consequence of this decoupling, distinguishing the lightest MSSM Higgs boson in the large M_A limit from the Higgs boson of the Standard Model (SM) will be very difficult. Formally, the decoupling of all SUSY particles (including the radiative corrections) implies that in the effective low-energy theory, all observables tend to their SM values in the limit of large SUSY masses and large M_A. It has been shown that all of the SUSY particles in the MSSM, including the heavy Higgs bosons H^0, A^0 and $H^\pm$, decouple at one-loop order from the low-energy electroweak gauge boson physics [2]. In particular, the contributions of the SUSY particles to low-energy processes either fall as inverse powers of the SUSY mass parameters or can be absorbed into counterterms for the tree-level couplings of the low-energy theory [3]. As a result, the radiative corrections involving SUSY particles go to zero in the asymptotic large SUSY mass limit. Our aim is to determine the nature of the decoupling limit at one-loop for the couplings of h^0 to SM particles.

In this paper, we focus on the h^0 coupling to $b\bar{b}$. This coupling determines the partial width of $h^0 \to b\bar{b}$, which is by far the dominant decay mode of h^0 in most of the MSSM parameter space. Because this decay is dominant, accurate knowledge of the $h^0 b\bar{b}$ coupling is very important for Higgs boson

searches. At LEP and the Tevatron, the primary Higgs search channel is $h^0 \to b\bar{b}$. The experimental reach of Higgs boson searches at the upcoming Tevatron Run 2 depends critically on the $h^0 \to b\bar{b}$ branching ratio [4]. In contrast, the Higgs boson searches at LEP do not depend as critically on the $h^0 \to b\bar{b}$ decay. At LEP, there is sufficient cross-section to detect the Higgs boson in multiple channels. Moreover, even without observing the Higgs decay products, the Higgs boson mass can be reconstructed by detecting the recoiling Z boson in $e^+e^- \to Zh^0$. At the CERN LHC, the primary Higgs search channel in the mass region below 130 GeV is the rare decay $h^0 \to \gamma\gamma$. The Higgs event rate in this channel is affected strongly if the total width of h^0 is modified due to corrections to the dominant $b\bar{b}$ decay mode [5]. The same holds true for other search channels at the LHC such as $h^0 \to \tau^+\tau^-$ [6].

In this paper we study the MSSM radiative corrections to the $h^0 b\bar{b}$ coupling at one loop, to leading order in α_s, and we analyze in detail their behavior in the decoupling limit.[1] These corrections are due to the SUSY-QCD (SQCD) sector and arise from gluino and bottom-squark (sbottom) exchange. Because of the dependence on the strong coupling constant, these are expected to be the most significant one-loop MSSM contributions over much of the MSSM parameter space. Potentially significant contributions can also arise from the SUSY-electroweak sector (the most significant of which are proportional to the Higgs-top quark Yukawa coupling); we will address these corrections elsewhere and do not consider them here.

The SQCD corrections to the $h^0 b\bar{b}$ coupling were first calculated using a diagrammatic approach in ref. [9] (which also contains results for the SUSY-electroweak corrections). These corrections have also been obtained in refs. [7,10]. The SQCD corrections were also computed in an effective Lagrangian approach in ref. [4], using the SUSY contributions to the b–quark self energy obtained in refs. [11,12] and neglecting terms suppressed by inverse powers of SUSY masses.

The radiatively-corrected $h^0 b\bar{b}$ coupling depends on the CP-even Higgs mixing angle α. At tree-level, this mixing angle is determined by fixing $\tan\beta$ and M_A. At one-loop order, there are no $\mathcal{O}(\alpha_s)$ corrections to this mixing angle. As a result, working to leading order in α_s, we may employ tree-level relations for α in our computation of the $h^0 b\bar{b}$ coupling. This procedure is no longer adequate once one-loop SUSY-electroweak effects are included. In the latter case, the one-loop radiative corrections to α must be taken into account, as described in refs. [4,5,13]. These papers show that the interplay between the radiative corrections to the mixing angle and to the $h^0 b\bar{b}$ coupling can be very important for Higgs collider phenomenology, particularly in the case when the branching ratio for $h^0 \to b\bar{b}$ is suppressed.[2] This is most easily seen as follows. When radiative corrections to the mixing angle α

[1] The radiatively-corrected $h^0 b\bar{b}$ coupling in the decoupling limit has also been considered previously in refs. [4,7,8].

[2] The relevance of the suppressed $h^0 b\bar{b}$ coupling for phenomenology has also been emphasized in refs. [8,14,15].

are included, it becomes possible to tune this angle to zero independent of the value of $\tan\beta$ by varying the SUSY parameters. At $\alpha = 0$, the tree-level couplings of h^0 to $b\bar{b}$ and $\tau^+\tau^-$ vanish, as do the ordinary QCD corrections [16] to the $h^0 b\bar{b}$ coupling. However, because the SQCD corrections to the $h^0 b\bar{b}$ coupling include contributions from diagrams involving the h^0 coupling to sbottoms, they remain nonzero at $\alpha = 0$. As a result, the $h^0\tau^+\tau^-$ coupling goes to zero at a different point in SUSY parameter space than the $h^0 b\bar{b}$ coupling does [5, 8, 13]. We will come back to these issues and study the approach to decoupling of the SUSY-electroweak corrections in a later paper.

In some regions of the MSSM parameter space, the SQCD corrections to the $h^0 b\bar{b}$ coupling become so large that it is important to take into account higher-order corrections. This has been carried out in refs. [17, 18] by resumming the leading $\tan\beta$ contributions to all orders of perturbation theory using an effective Lagrangian approach. This resummation is not important in our present work because we are interested in the decoupling limit in which the one-loop corrections to the $h^0 b\bar{b}$ coupling are small.

In this paper we analyze the full diagrammatic formulae for the on-shell one-loop SQCD corrections to the $h^0 b\bar{b}$ coupling. We perform expansions in inverse powers of SUSY masses in order to examine the decoupling behavior when the SUSY masses are large compared to M_Z. The SQCD corrections depend on a number of different SUSY mass parameters, and the relative sizes of these masses affect the manifestation of the decoupling. To remain as model-independent as possible, we make no assumptions about relations among the SUSY parameters that may arise from grand unification or specific SUSY-breaking scenarios. We consider the soft-SUSY-breaking parameters and the μ parameter to be independent parameters whose magnitudes are all of order 1 TeV.

In this paper, we demonstrate that in the limit of large M_A (in this limit one also has $M_{H^0}, M_{H^\pm} \gg M_Z$) and large sbottom and gluino masses ($M_{\tilde{b}_i}, M_{\tilde{g}} \gg M_Z$), the SM expression for the $h^0 b\bar{b}$ one-loop coupling is recovered. That is, the SQCD corrections to the $h^0 b\bar{b}$ coupling decouple in the limit of large SUSY masses and large M_A. In particular, we examine the case of large $\tan\beta$, for which the SQCD corrections are enhanced. This enhancement can delay the onset of decoupling and give rise to a significant one-loop correction, even for moderate to large values of the SUSY masses.

This paper is organized as follows. In Section 2 we define our notation and briefly review the Higgs and sbottom sectors of the MSSM. In Section 3 we give the exact one loop formula for the SQCD corrections to the $h^0 b\bar{b}$ coupling. In Section 4 we derive analytic expressions for the SQCD corrections in the limit of large SUSY masses. We analyze the decoupling of the SQCD corrections for various hierarchies of mass parameters, and numerically compare the analytic approximations to the exact one-loop result. In Section 5 we summarize our conclusions. Finally, the Appendix contains expansions of the one-loop integrals used in our calculations.

2 Higgs and sbottom masses in the MSSM

In the MSSM, the parameters of the Higgs sector are constrained at tree-level in such a way that the Higgs masses and mixing angles depend on only two unknown parameters. These are commonly chosen to be the mass of the CP-odd neutral Higgs boson A^0 and the ratio of the vacuum expectation values (vevs) of the two Higgs doublets, $\tan\beta = v_2/v_1$. (For a review of the MSSM Higgs sector, see [19].) In terms of these parameters, the mass of the charged Higgs boson $H^\pm$ at tree level is $M_{H^\pm}^2 = M_A^2 + M_W^2$, and the masses of the CP-even neutral Higgs bosons h^0 and H^0 are obtained by diagonalizing the tree-level mass-squared matrix,

$$\mathcal{M}^2 = \begin{pmatrix} M_A^2 \sin^2\beta + M_Z^2 \cos^2\beta & -(M_A^2 + M_Z^2)\sin\beta\cos\beta \\ -(M_A^2 + M_Z^2)\sin\beta\cos\beta & M_A^2\cos^2\beta + M_Z^2\sin^2\beta \end{pmatrix} . \tag{2.1}$$

The eigenvalues of this matrix are,

$$M_{H^0,h^0}^2 = \frac{1}{2}\left[M_A^2 + M_Z^2 \pm \sqrt{(M_A^2+M_Z^2)^2 - 4M_A^2M_Z^2\cos^2 2\beta}\right] , \tag{2.2}$$

with $M_{h^0} < M_{H^0}$. At tree-level, $M_{h^0} \leq M_Z|\cos 2\beta|$; this bound is saturated at large M_A. We choose a convention where the vevs are positive so that $0 < \beta < \pi/2$. The mixing angle that diagonalizes $\mathcal{M}^2$ is given at tree-level by

$$\tan 2\alpha = \tan 2\beta \, \frac{M_A^2 + M_Z^2}{M_A^2 - M_Z^2} . \tag{2.3}$$

In the conventions employed here, $-\pi/2 < \alpha < 0$ (see ref. [20] for further details). From the above results it is easy to obtain:

$$\cos^2(\beta-\alpha) = \frac{M_{h^0}^2(M_Z^2 - M_{h^0}^2)}{M_A^2(M_{H^0}^2 - M_{h^0}^2)} . \tag{2.4}$$

In the limit of $M_A \gg M_Z$, the expressions for the Higgs masses and mixing angle simplify and one finds

$$\begin{aligned} M_{h^0}^2 &\simeq M_Z^2\cos^2 2\beta , \\ M_{H^0}^2 &\simeq M_A^2 + M_Z^2\sin^2 2\beta , \\ \cos^2(\beta-\alpha) &\simeq \frac{M_Z^4 \sin^2 4\beta}{4M_A^4} . \end{aligned} \tag{2.5}$$

Two consequences are immediately apparent. First, $M_A \simeq M_{H^0} \simeq M_{H^\pm}$, up to corrections of $\mathcal{O}(M_Z^2/M_A)$. Second, $\cos(\beta-\alpha) = 0$ up to corrections of $\mathcal{O}(M_Z^2/M_A^2)$. This limit is known as the decoupling limit because when M_A is large, one can define an effective low-energy theory below the scale of M_A in which the effective Higgs sector consists only of one light CP-even Higgs

boson, h^0, whose couplings to Standard Model particles are indistinguishable from those of the SM Higgs boson [1]. From eq. 2.5, one can easily derive:

$$\cot\alpha = -\tan\beta - \frac{2M_Z^2}{M_A^2}\tan\beta\cos 2\beta + \mathcal{O}\left(\frac{M_Z^4}{M_A^4}\right). \tag{2.6}$$

When radiative corrections to the CP-even Higgs mass-squared matrix are taken into account, the upper bound on M_{h^0} increases substantially to $M_{h^0} \lesssim 135$ GeV (assuming all supersymmetric particles are no heavier than about 1 TeV), and corrections to α become substantial for low M_A. These corrections are well known [12, 21–26] and the leading contributions have been computed up to two-loop order. In this paper we consider only the contributions to the $h^0 b\bar{b}$ coupling of order α_s at one loop. Because the $\mathcal{O}(\alpha_s)$ contributions to the CP-even Higgs mass-squared matrix only first arise at the two-loop level, the radiative corrections to this matrix are irrelevant to our present work. (In contrast, they do contribute to the one-loop SUSY-electroweak corrections to the $h^0 b\bar{b}$ coupling.)

From direct searches at LEP the MSSM h^0 and A^0 masses are constrained to be $M_{h^0} > 88.3$ GeV and $M_A > 88.4$ GeV [27]. For a range of values of $\tan\beta$ close to one, the theoretical upper bound on M_{h^0} is lower than the experimental lower bound, so the corresponding region of $\tan\beta$ can be ruled out. Because of the radiative corrections, the variation of the upper bound depends primarily on the precise value of the top quark mass and the mixing in the stop sector. For the conservative choice of $m_t < 179.4$ GeV and mixing in the stop sector that maximizes the upper bound on M_{h^0}, values of $\tan\beta$ between 0.8 and 1.5 are excluded [27].

We now discuss the parameters of the sbottom sector. The tree-level sbottom squared-mass matrix is:

$$\mathcal{M}_{\tilde{b}}^2 = \begin{pmatrix} M_L^2 & m_b X_b \\ m_b X_b & M_R^2 \end{pmatrix}, \tag{2.7}$$

where we use the notation,

$$\begin{aligned} X_b &= A_b - \mu\tan\beta\,, \\ M_L^2 &= M_{\tilde{Q}}^2 + m_b^2 + M_Z^2(I_3^b - Q_b s_W^2)\cos 2\beta\,, \\ M_R^2 &= M_{\tilde{D}}^2 + m_b^2 + M_Z^2 Q_b s_W^2 \cos 2\beta\,. \end{aligned} \tag{2.8}$$

Here $I_3^b = -1/2$ and $Q_b = -1/3$ are the isospin and electric charge of the b-quark, respectively and $s_W \equiv \sin\theta_W$. The parameters $M_{\tilde{Q}}$ and $M_{\tilde{D}}$ are the soft-SUSY-breaking masses for the third-generation SU(2) squark doublet $\tilde{Q} = (\tilde{t}_L, \tilde{b}_L)$ and the singlet $\tilde{D} = \tilde{b}_R^*$, respectively. A_b is a soft-SUSY-breaking trilinear coupling and μ is the bilinear coupling of the two Higgs doublet superfields. The sbottom mass eigenstates are

$$\tilde{b}_1 = \cos\theta_{\tilde{b}}\,\tilde{b}_L + \sin\theta_{\tilde{b}}\,\tilde{b}_R\,; \qquad \tilde{b}_2 = -\sin\theta_{\tilde{b}}\,\tilde{b}_L + \cos\theta_{\tilde{b}}\,\tilde{b}_R\,, \tag{2.9}$$

where $-\pi/4 \leq \theta_{\tilde{b}} \leq \pi/4$ is defined so that $\tilde{b}_1$ ($\tilde{b}_2$) is predominantly $\tilde{b}_L$ ($\tilde{b}_R$). The sbottom mass eigenvalues are then given by

$$M^2_{\tilde{b}_{1,2}} = \frac{1}{2}\left[M_L^2 + M_R^2 \pm \sigma_{LR}\sqrt{(M_L^2 - M_R^2)^2 + 4m_b^2 X_b^2}\right], \tag{2.10}$$

where[3]

$$\sigma_{LR} \equiv \mathrm{sgn}(M_L^2 - M_R^2), \tag{2.11}$$

and the mixing angle $\theta_{\tilde{b}}$ is given by

$$\begin{aligned} \cos 2\theta_{\tilde{b}} &= \frac{M_L^2 - M_R^2}{M^2_{\tilde{b}_1} - M^2_{\tilde{b}_2}}, \\ \sin 2\theta_{\tilde{b}} &= \frac{2m_b X_b}{M^2_{\tilde{b}_1} - M^2_{\tilde{b}_2}}. \end{aligned} \tag{2.12}$$

Note that in our conventions, $M_{\tilde{b}_1} > M_{\tilde{b}_2}$ if $\sigma_{LR} > 0$, whereas the order of the sbottom masses switches if $\sigma_{LR} < 0$.

From direct searches at the Tevatron [28], the sbottoms must be heavier than about 140 GeV, assuming that the mass of the lightest neutralino $\tilde{\chi}_1^0$ is less than half the mass of the lighter sbottom. For heavier neutralinos, the Tevatron searches lose efficiency. In this region the direct searches at LEP [29] place a lower bound on the sbottom masses of about 85 GeV. The LEP bounds are valid only for $\tilde{b} - \tilde{\chi}_1^0$ mass splittings larger than about 5 GeV, so that the decay mode $\tilde{b} \to b\tilde{\chi}_1^0$ is kinematically accessible.

The limits on the gluino mass $M_{\tilde{g}}$ are more model-dependent. If one assumes relations between the gaugino masses such that they unify at the GUT scale, then $M_{\tilde{g}}$ is constrained from direct searches at the Tevatron to be greater than 173 GeV, independent of the squark masses [30].

3 SQCD corrections to $h^0 \to b\bar{b}$

The $h^0 b\bar{b}$ coupling is given at one-loop level to order α_s by

$$\bar{g}_{hbb} = g_{hbb} + \delta g_{hbb}^{QCD} + \delta g_{hbb}^{SQCD} \equiv g_{hbb}\left(1 + \Delta_{QCD} + \Delta_{SQCD}\right), \tag{3.1}$$

where $\bar{g}_{hbb}$ is the one-loop coupling, g_{hbb} is the tree-level coupling, δg_{hbb}^{QCD} is the radiative correction from pure QCD [16], and δg_{hbb}^{SQCD} is the one-loop SQCD contribution.

The tree-level $h^0 b\bar{b}$ coupling is given by

$$g_{hbb} = \frac{g m_b \sin\alpha}{2 M_W \cos\beta}. \tag{3.2}$$

[3]If $M_L = M_R$, then σ_{LR} is not well-defined. In the present context, a useful convention is to set $\sigma_{LR} = \sigma_X$ [where $\sigma_X \equiv \mathrm{sgn}(X_b)$] if $M_L = M_R$. Nevertheless, one can check that our final expressions for the radiative corrections in Section 4 are independent of this choice.

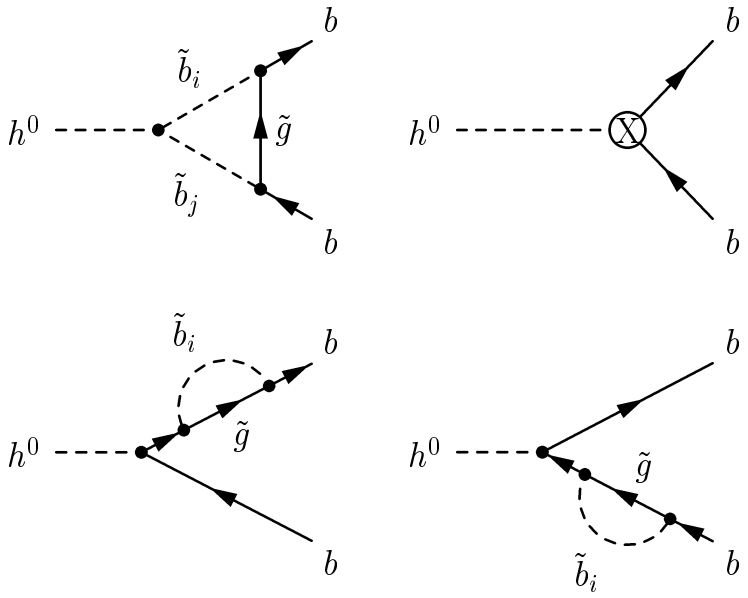

Figure 1: Feynman diagrams for the SQCD corrections to the $h^0 b\bar{b}$ coupling. The vertex marked with the X refers to the one-loop $h^0 b\bar{b}$ counterterm.

Note that in the limit of large M_A, $\sin\alpha \to -\cos\beta$ and g_{hbb} tends to the SM coupling, $g_{hbb}^{SM} = -gm_b/(2M_W)$. The one-loop corrections to the $h^0 b\bar{b}$ coupling modify the $h^0 \to b\bar{b}$ decay width as follows, keeping only correction terms of $\mathcal{O}(\alpha_s)$:

$$\bar{\Gamma}(h^0 \to b\bar{b}) = \Gamma(h^0 \to b\bar{b})(1 + 2\Delta_{QCD} + 2\Delta_{SQCD})\,, \tag{3.3}$$

where $\bar{\Gamma}$ is the one-loop partial width and Γ is the tree-level partial width.

The SQCD contribution to the $h^0 b\bar{b}$ coupling comes from diagrams involving the exchange of virtual gluinos ($\tilde{g}$) and sbottoms ($\tilde{b_i}$), as shown in fig. 1. We have

$$\delta g_{hbb}^{SQCD} = (\delta g_{hbb})_3^{SQCD} + (\delta g_{hbb})_2^{SQCD} + (\delta g_{hbb})_{\rm X}^{SQCD}\,, \tag{3.4}$$

consisting of contributions from the vertex correction, the b-quark wave function renormalization, and the counterterm from the renormalization of the b-quark Yukawa coupling, respectively. To compute the one-loop Yukawa counterterm contribution, we note that the Higgs wave function, the vevs (and hence $\tan\beta$) and the parameters g, M_W and α receive no $\mathcal{O}(\alpha_s)$ corrections at one-loop. Thus, to leading order in α_s, $(\delta g_{hbb})_{\rm X}^{SQCD}$ can be easily obtained from eq. 3.2 and depends only on the b-quark mass counterterm as follows:

$$(\delta g_{hbb})_{\rm X}^{SQCD} = g_{hbb}\,\frac{(\delta m_b)^{SQCD}}{m_b}\,. \tag{3.5}$$

In eq. 3.5, $(\delta m_b)^{SQCD}$ is the SQCD contribution to the b-quark mass counterterm, which is fixed by defining m_b to be the pole of the one-loop $\mathcal{O}(\alpha_s)$

b-quark propagator. This is the on-shell renormalization scheme.

We have computed the various contributions to δg_{hbb}^{SQCD} [see eq. 3.4]. The contribution of the one-loop vertex is given by:

$$\begin{aligned}
\frac{(\delta g_{hbb})_3^{SQCD}}{g_{hbb}} = \frac{\alpha_s}{3\pi}\Bigg\{ & \left[\frac{2M_Z^2}{m_b}\frac{\cos\beta\sin(\alpha+\beta)}{\sin\alpha}(I_3^b c_b^2 - Q_b s_W^2 c_{2b}) + 2m_b + Y_b s_{2b}\right] \\
& \times \left[m_b C_{11} + M_{\tilde{g}} s_{2b} C_0\right](m_b^2, M_{h^0}^2, m_b^2; M_{\tilde{g}}^2, M_{\tilde{b}_1}^2, M_{\tilde{b}_1}^2) \\
& + \left[\frac{2M_Z^2}{m_b}\frac{\cos\beta\sin(\alpha+\beta)}{\sin\alpha}(I_3^b s_b^2 + Q_b s_W^2 c_{2b}) + 2m_b - Y_b s_{2b}\right] \\
& \times \left[m_b C_{11} - M_{\tilde{g}} s_{2b} C_0\right](m_b^2, M_{h^0}^2, m_b^2; M_{\tilde{g}}^2, M_{\tilde{b}_2}^2, M_{\tilde{b}_2}^2) \\
& + \left[-\frac{M_Z^2}{m_b}\frac{\cos\beta\sin(\alpha+\beta)}{\sin\alpha}(I_3^b - 2Q_b s_W^2)s_{2b} + Y_b c_{2b}\right] \\
& \times \left[2M_{\tilde{g}} c_{2b} C_0(m_b^2, M_{h^0}^2, m_b^2; M_{\tilde{g}}^2, M_{\tilde{b}_1}^2, M_{\tilde{b}_2}^2)\right]\Bigg\}, \qquad (3.6)
\end{aligned}$$

where $c_b \equiv \cos\theta_{\tilde{b}}$, $c_{2b} \equiv \cos 2\theta_{\tilde{b}}$, $s_b \equiv \sin\theta_{\tilde{b}}$, *etc.*, and Y_b arises in the Higgs coupling to sbottoms:

$$Y_b \equiv A_b + \mu\cot\alpha\,. \qquad (3.7)$$

The contribution from the b-quark self-energy and the $h^0 b\bar{b}$ vertex counterterm is given by

$$\begin{aligned}
\frac{(\delta g_{hbb})_2^{SQCD} + (\delta g_{hbb})_{\rm X}^{SQCD}}{g_{hbb}} = & \\
& -\frac{\alpha_s}{3\pi}\Bigg\{\frac{M_{\tilde{g}}}{m_b}s_{2b}\left[B_0(m_b^2; M_{\tilde{g}}^2, M_{\tilde{b}_1}^2) - B_0(m_b^2; M_{\tilde{g}}^2, M_{\tilde{b}_2}^2)\right] \\
& -2m_b^2\left[B_1'(m_b^2; M_{\tilde{g}}^2, M_{\tilde{b}_1}^2) + B_1'(m_b^2; M_{\tilde{g}}^2, M_{\tilde{b}_2}^2)\right] \\
& -2m_b M_{\tilde{g}} s_{2b}\left[B_0'(m_b^2; M_{\tilde{g}}^2, M_{\tilde{b}_1}^2) - B_0'(m_b^2; M_{\tilde{g}}^2, M_{\tilde{b}_2}^2)\right]\Bigg\}. \qquad (3.8)
\end{aligned}$$

Our notation for the loop integrals B_0, B_0', B_1', C_0 and C_{11} is defined in the Appendix. We have checked that our results are in agreement with the calculations of ref. [9].

4 Analytic and numerical results

We now analyze the decoupling behavior of the SQCD corrections to the $h^0 b\bar{b}$ coupling. We derive approximate analytic expressions for the SQCD corrections in the limit of large SUSY mass parameters and explore the nature of the decoupling limit.

We define our expansion parameters as follows. Since we are interested in the limit of large SUSY mass parameters, we consider all the soft-SUSY-breaking mass parameters and the μ parameter to be of the same order (collectively denoted by M_{SUSY}) and much heavier than the electroweak scale. That is,

$$M_{SUSY} \sim M_L \sim M_R \sim M_{\tilde{g}} \sim \mu \sim A_b \gg M_{EW}, \tag{4.1}$$

where M_L and M_R are defined in eq. 2.8. We give expansions of the SQCD corrections to the $h^0 b\bar{b}$ coupling in inverse powers of the SUSY mass parameters, up to order M_{EW}^2/M_{SUSY}^2. We consider M_Z, M_{h^0}, $m_b \tan\beta$, and $m_b \cot\alpha$ to all be of order M_{EW}. We neglect small contributions of order m_b^2/M_{SUSY}^2 and $m_b M_{EW}/M_{SUSY}^2$ that are not enhanced by $\tan\beta$ or $\cot\alpha$. The expansions of the loop integrals are given in the Appendix. There are two possible extreme configurations of the sbottom mass-squared matrix that we must separately consider: maximal and near-zero mixing.

Maximal mixing ($\theta_{\tilde{b}} \simeq \pm\pi/4$) between $\tilde{b}_L$ and $\tilde{b}_R$ arises when the splitting between the diagonal elements of the mass-squared matrix is small compared to the off-diagonal elements: $|M_L^2 - M_R^2| \ll m_b|X_b|$. Because of the $\tan\beta$ enhancement in X_b, $m_b X_b$ is of order $M_{EW} M_{SUSY}$. In this case we consider $|M_L^2 - M_R^2|$ to be of order M_{EW}^2, so that the mass splitting between the two sbottoms is small compared to their masses and we must take care to treat it properly in the expansions. We consider this case in Section 4.1.

Near-zero mixing between $\tilde{b}_L$ and $\tilde{b}_R$ arises when the splitting between the diagonal elements of the mass-squared matrix is large compared to the off-diagonal elements, $|M_L^2 - M_R^2| \gg m_b|X_b|$. This is the case usually considered in the literature, because M_L and M_R depend on two different soft-SUSY-breaking parameters $M_{\tilde{Q}}$ and $M_{\tilde{D}}$, respectively, and the b-quark mass in the off-diagonal elements is small. In this case the mass splitting between the two sbottoms will be of the same order as their masses (*i.e.*, $|M_L^2 - M_R^2|$ is of order M_{SUSY}^2) and this has to be treated properly in the expansions. We consider this case in Section 4.2.

4.1 Maximal $\tilde{b}_L - \tilde{b}_R$ mixing

Maximal mixing in the sbottom sector arises when $|M_L^2 - M_R^2| \ll m_b|X_b|$. In this limit, we can expand the sbottom mass-squared eigenvalues in powers of the small parameter $(M_L^2 - M_R^2)/m_b X_b$ (which is of order M_{EW}/M_{SUSY}) as follows:

$$M_{\tilde{b}_{1,2}}^2 \simeq M_S^2 \pm \Delta^2\,, \tag{4.2}$$

where we have defined

$$\begin{aligned} M_S^2 &= \tfrac{1}{2}(M_L^2 + M_R^2) = \tfrac{1}{2}(M_{\tilde{b}_1}^2 + M_{\tilde{b}_2}^2) \\ \Delta^2 &= \sigma_{LR} m_b |X_b| \left[1 + \frac{(M_L^2 - M_R^2)^2}{8 m_b^2 X_b^2}\right]. \end{aligned} \tag{4.3}$$

Here M_S^2 is of order M_{SUSY}^2 while Δ^2 is of order $M_{EW}M_{SUSY}$. Expanding the expressions for the mixing angle in terms of the same small parameter, we obtain

$$\cos 2\theta_{\tilde{b}} \simeq \left| \frac{M_L^2 - M_R^2}{2m_b X_b} \right| ,$$
$$\sin 2\theta_{\tilde{b}} \simeq \sigma_{LR}\sigma_X \left[1 - \frac{(M_L^2 - M_R^2)^2}{8m_b^2 X_b^2} \right] , \qquad (4.4)$$

where $\sigma_X \equiv \mathrm{sgn}(X_b)$. Expanding eqs. 3.6 and 3.8 to order M_{EW}^2/M_{SUSY}^2, we find

$$\Delta_{SQCD} = \frac{\alpha_s}{3\pi} \left\{ \frac{-\mu M_{\tilde{g}}}{M_S^2} (\tan\beta + \cot\alpha) f_1(R) - \frac{Y_b M_{\tilde{g}} M_{h^0}^2}{12 M_S^4} f_4(R) \right.$$
$$+ \frac{\mu^2 m_b^2 \tan^2\beta}{2M_S^4} \left[\frac{\cot\alpha}{\tan\beta} f_4(R) - \frac{M_{\tilde{g}}}{M_S^2} \left(Y_b - 2A_b \frac{\cot\alpha}{\tan\beta} \right) f_3(R) \right]$$
$$\left. + \frac{2}{3} \frac{M_Z^2}{M_S^2} \frac{\cos\beta \sin(\alpha+\beta)}{\sin\alpha} I_3^b \left(f_5(R) + \frac{M_{\tilde{g}} X_b}{M_S^2} f_2(R) \right) + \mathcal{O}\left(\frac{m_b M_{EW}}{M_{SUSY}^2} \right) \right\} , \qquad (4.5)$$

where $R \equiv M_{\tilde{g}}/M_S$. The functions $f_i(R)$ arise from the expansions of the loop integrals and are given in the Appendix. They are normalized so that $f_i(1) = 1$. Note that terms of order $(M_L^2 - M_R^2)^2/(m_b^2 X_b^2)$ cancel exactly in the leading order of the large M_{SUSY} expansion [eq. 4.5].

The first term in eq. 4.5 is zeroth order in M_{SUSY}. That is, if the ratios between the SUSY parameters are fixed and the SUSY mass scale is taken arbitrarily heavy, this term remains constant. This non-decoupling behavior has been pointed out previously in refs. [4, 5]. If the SUSY mass scale is much larger than M_A, then one may define a low-energy effective theory by integrating out the SUSY particles. This low-energy effective theory contains two Higgs doublets, whose couplings to fermions are unrestricted (*i.e.*, each Higgs doublet couples to *both* up-type and down-type quarks), characteristic of the so-called general type-III model [31].

The remaining terms are of order M_{EW}^2/M_{SUSY}^2. In contrast to the first term, they depend on A_b (through X_b and Y_b). However, the contribution proportional to A_b is not enhanced when $\tan\beta$ (or $\cot\alpha$) is large, and so is less significant at large $\tan\beta$ than the contribution proportional to μ. Neglecting all terms that are not enhanced by large $\tan\beta$ or $\cot\alpha$, we find that Δ_{SQCD} is proportional to the product $\mu M_{\tilde{g}}$. Because of this, for large $\tan\beta$ the sign of Δ_{SQCD} can be used as a test of the anomaly-mediated SUSY breaking scenario [32], which predicts a negative $M_{\tilde{g}}$ [33]. Of course, the sign of μ must be determined from another SUSY process for the sign of $M_{\tilde{g}}$ to be extracted.

4.2 Near-zero $\tilde{b}_L - \tilde{b}_R$ mixing

Near-zero mixing in the sbottom sector arises when $|M_L^2 - M_R^2| \gg m_b|X_b|$. This corresponds to taking the difference between the physical sbottom masses to be of the same order as the masses themselves. In this case we write our results in terms of the physical sbottom masses and expand in powers of the small parameter $m_b X_b/(M^2_{\tilde{b}_1} - M^2_{\tilde{b}_2})$, which we take to be of order M_{EW}/M_{SUSY}. The mixing angle is then given by eq. 2.12, from which one easily derives the expansion

$$\cos 2\theta_{\tilde{b}} \simeq 1 - \frac{2m_b^2 X_b^2}{(M^2_{\tilde{b}_1} - M^2_{\tilde{b}_2})^2}. \tag{4.6}$$

Expanding eqs. 3.6 and 3.8 to order M^2_{EW}/M^2_{SUSY}, and writing the result in terms of the physical sbottom masses, we find:

$$\begin{aligned}
\Delta_{SQCD} = \frac{\alpha_s}{3\pi}\Bigg\{ & \frac{-2\mu M_{\tilde{g}}}{M^2_{\tilde{b}_1} - M^2_{\tilde{b}_2}}(\tan\beta + \cot\alpha)\, h_1(R_1,R_2) + 2M^2_{h^0}\frac{M_{\tilde{g}} Y_b\, h_2(R_1,R_2)}{(M^2_{\tilde{b}_1} - M^2_{\tilde{b}_2})^2} \\
& + 2M_Z^2 \frac{\cos\beta\sin(\alpha+\beta)}{\sin\alpha}\Bigg[(I_3^b - Q_b s_W^2)\left(\frac{f_5(R_1)}{3M^2_{\tilde{b}_1}} - \frac{M_{\tilde{g}}X_b}{M^2_{\tilde{b}_1} - M^2_{\tilde{b}_2}}\frac{f_1(R_1)}{M^2_{\tilde{b}_1}} \right. \\
& \qquad \left. + \frac{2M_{\tilde{g}}X_b\, h_1(R_1,R_2)}{(M^2_{\tilde{b}_1} - M^2_{\tilde{b}_2})^2}\right) \\
& \qquad + Q_b s_W^2\left(\frac{f_5(R_2)}{3M^2_{\tilde{b}_2}} + \frac{M_{\tilde{g}}X_b}{M^2_{\tilde{b}_1} - M^2_{\tilde{b}_2}}\frac{f_1(R_2)}{M^2_{\tilde{b}_2}} - \frac{2M_{\tilde{g}}X_b\, h_1(R_1,R_2)}{(M^2_{\tilde{b}_1} - M^2_{\tilde{b}_2})^2}\right)\Bigg] \\
& - \frac{2\mu^2 M_{\tilde{g}} m_b^2 \tan^2\beta}{(M^2_{\tilde{b}_1} - M^2_{\tilde{b}_2})^2}\left(Y_b - 2A_b\frac{\cot\alpha}{\tan\beta}\right)\left(\frac{f_1(R_1)}{M^2_{\tilde{b}_1}} + \frac{f_1(R_2)}{M^2_{\tilde{b}_2}} - \frac{4h_1(R_1,R_2)}{M^2_{\tilde{b}_1} - M^2_{\tilde{b}_2}}\right) \\
& - \frac{2\mu^2 m_b^2 \tan\beta\cot\alpha}{M^2_{\tilde{b}_1} - M^2_{\tilde{b}_2}}\left(\frac{f_5(R_1)}{3M^2_{\tilde{b}_1}} - \frac{f_5(R_2)}{3M^2_{\tilde{b}_2}}\right) + \mathcal{O}\left(\frac{m_b M_{EW}}{M^2_{SUSY}}\right)\Bigg\}\,,
\end{aligned} \tag{4.7}$$

where $R_i \equiv M_{\tilde{g}}/M_{\tilde{b}_i}$ $(i = 1, 2)$. The functions $h_i(R_1, R_2)$ and $f_{1,5}(R_i)$ arise from the expansions of the loop integrals and are given in the Appendix.

As in the case of maximal sbottom mixing, the first term in eq. 4.7 is zeroth order in M_{SUSY}. The remaining terms are of order M^2_{EW}/M^2_{SUSY}. As in the previous section, if we neglect all terms that are not enhanced by large $\tan\beta$ or $\cot\alpha$, we find that the dependence on A_b drops out and Δ_{SQCD} is again proportional to the product $\mu M_{\tilde{g}}$.

4.3 The approach to the decoupling limit

If we take all SUSY mass parameters large at fixed M_A in eqs. 4.5 and 4.7, then Δ_{SQCD} tends to a nonzero constant; *i.e.*, the SQCD corrections do

not decouple. However, we are especially interested in the case where both M_{SUSY} and M_A are large. In eqs. 4.5 and 4.7, the terms of zeroth order in M_{SUSY} are proportional to $\tan\beta + \cot\alpha$. From eq. 2.6,

$$\tan\beta + \cot\alpha = -\frac{2M_Z^2}{M_A^2}\tan\beta\cos 2\beta + \mathcal{O}\left(\frac{M_{EW}^4}{M_A^4}\right). \tag{4.8}$$

Thus, the first term in eq. 4.5 and in eq. 4.7 is of order $M_{EW}^2\tan\beta/M_A^2$, and therefore decouples in the limit of large M_A. However, the approach to decoupling is delayed in the large $\tan\beta$ regime.[4] Specifically, for values of $M_A^2 \sim M_Z^2\tan\beta$, we see that $\tan\beta + \cot\alpha \sim \mathcal{O}(1)$. For example, if $\tan\beta \sim 50$, then even for values of $M_A \sim 1$ TeV, decoupling has not yet set in.

Other terms in eqs. 4.5 and 4.7 also exhibit delayed decoupling. In particular, eq. 4.8 implies that

$$Y_b = X_b + \mathcal{O}\left(\frac{M_{SUSY}M_{EW}^2\tan\beta}{M_A^2}\right), \tag{4.9}$$

so that Y_b is also enhanced at large $\tan\beta$. Hence, all terms in eqs. 4.5 and 4.7 that are proportional to either X_b or Y_b are of order $M_{EW}^2\tan\beta/M_{SUSY}^2$. Again, if $\tan\beta \sim 50$ and $M_{SUSY} \sim 1$ TeV, decoupling has not yet set in.

The remaining terms in eqs. 4.5 and 4.7 exhibit the expected decoupling in the usual sense (with no delay). In particular, we may set $\alpha = \beta - \pi/2$ in the decoupling limit to obtain

$$\frac{\cos\beta\sin(\alpha+\beta)}{\sin\alpha} = \cos 2\beta + \mathcal{O}\left(\frac{M_{EW}^2}{M_A^2}\right), \tag{4.10}$$

which exhibits no $\tan\beta$ enhancement. All remaining factors of $\tan\beta$ are multiplied by the appropriate power of m_b, and since $m_b\tan\beta \sim M_{EW}$, no delayed decoupling results from these terms.

We have thus shown analytically that the one-loop SQCD corrections to the $h^0b\bar{b}$ coupling decouple in the limit of large M_{SUSY} and large M_A. The decoupling takes the generic form:

$$\Delta_{SQCD} \sim C_1\frac{M_{EW}^2}{M_A^2} + C_2\frac{M_{EW}^2}{M_{SUSY}^2}. \tag{4.11}$$

In general C_1 approaches a non-zero constant as $M_{SUSY} \to \infty$, while C_2 approaches a (different) non-zero constant as $M_A \to \infty$. Thus, the decoupling limit requires both M_A and M_{SUSY} to become simultaneously large (as compared to M_{EW}). However, we will demonstrate that in some cases the SQCD radiative corrections vanish in the limit where some SUSY particle masses are large, independent of the value of M_A.

This decoupling is shown numerically [5] in figs. 2 and 3. In fig. 2, we plot

[4] The enhancement of the radiatively-corrected $h^0b\bar{b}$ coupling at large $\tan\beta$ has also been emphasized in refs. [4, 7, 8, 10, 15].

[5] In our numerical analysis we have taken the b-quark pole-mass to be 4.75 GeV and $\alpha_s = 0.119$. Because of the experimental constraints on the sbottom masses, we consider only regions of parameter space in which both sbottoms are heavier than 100 GeV.

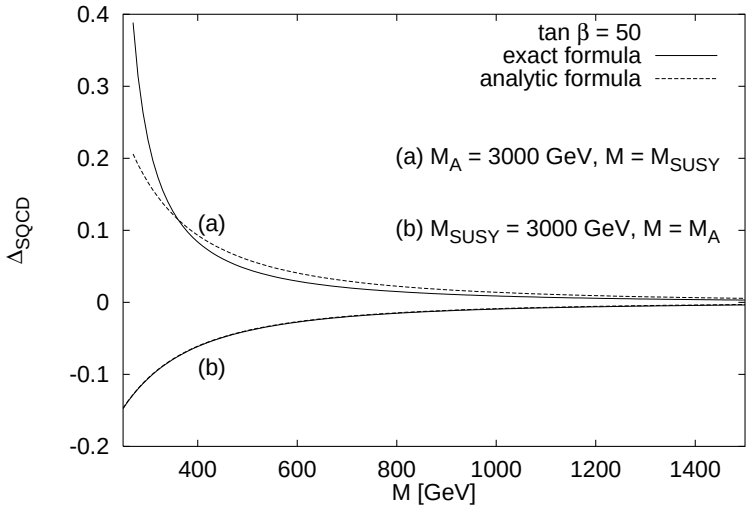

Figure 2: $\Delta_{\rm SQCD}$ as a function of particle mass for $\tan\beta = 50$ and $M_{SUSY} = M_L = M_R = M_S = M_{\tilde{g}} = \mu = A_b$. The curves (a) are plotted *vs.* M_{SUSY}, with $M_A = 3000$ GeV; whereas the curves (b) are plotted *vs.* M_A, with $M_{SUSY} = 3000$ GeV. Solid lines are based on the exact one-loop formula and dashed lines are based on the analytic approximation of eq. 4.5.

the exact one-loop expression for Δ_{SQCD} (solid lines) and the expansion of eq. 4.5 (dashed lines) for $\tan\beta = 50$ and $M_{SUSY} = M_L = M_R = M_S = M_{\tilde{g}} = \mu = A_b$. The lines labeled (a) show Δ_{SQCD} as a function of M_{SUSY}. We have fixed M_A very large, $M_A = 3000$ GeV, in order to eliminate the contribution to Δ_{SQCD} that decouples at large M_A. We use the exact tree-level formula for $\cot\alpha$ as a function of M_A and $\tan\beta$. The lines labeled (b) show Δ_{SQCD} as a function of M_A, where now we have fixed M_{SUSY} to be very large, $M_{SUSY} = 3000$ GeV, in order to examine only the contribution to Δ_{SQCD} that does not decouple at large M_{SUSY}. We note that for very large M_{SUSY} and $M_A = 1$ TeV, Δ_{SQCD} is of order -1% for $\tan\beta = 50$. We have plotted our results for $\mu M_{\tilde{g}}$ positive. In the approximation of neglecting terms not enhanced by large $\tan\beta$ or $\cot\alpha$, changing the sign of $\mu M_{\tilde{g}}$ simply flips the sign of Δ_{SQCD}.

In fig. 3 we again plot the exact one-loop expression for Δ_{SQCD} (solid lines) and the expansion of eq. 4.5 (dashed lines) for all the SUSY mass parameters equal, $M_{SUSY} = M_L = M_R = M_S = M_{\tilde{g}} = \mu = A_b$, and three values of $\tan\beta$. [6] Note the change in the vertical scale for the plots with different values of $\tan\beta$. We show the dependence of Δ_{SQCD} on M_{SUSY} (left-hand panels) and M_A (right-hand panels). Clearly, in the limit of large M_{SUSY}, Δ_{SQCD} tends to a non-vanishing constant, and this constant tends to zero in the large M_A limit. Similarly, in the limit of large M_A, Δ_{SQCD}

[6] Although we have chosen $M_L = M_R$ for simplicity, our results are not particularly sensitive to this choice as long as $|M_L^2 - M_R^2| \ll m_b|X_b|$ (*c.f.* the remarks below eq. 4.5).

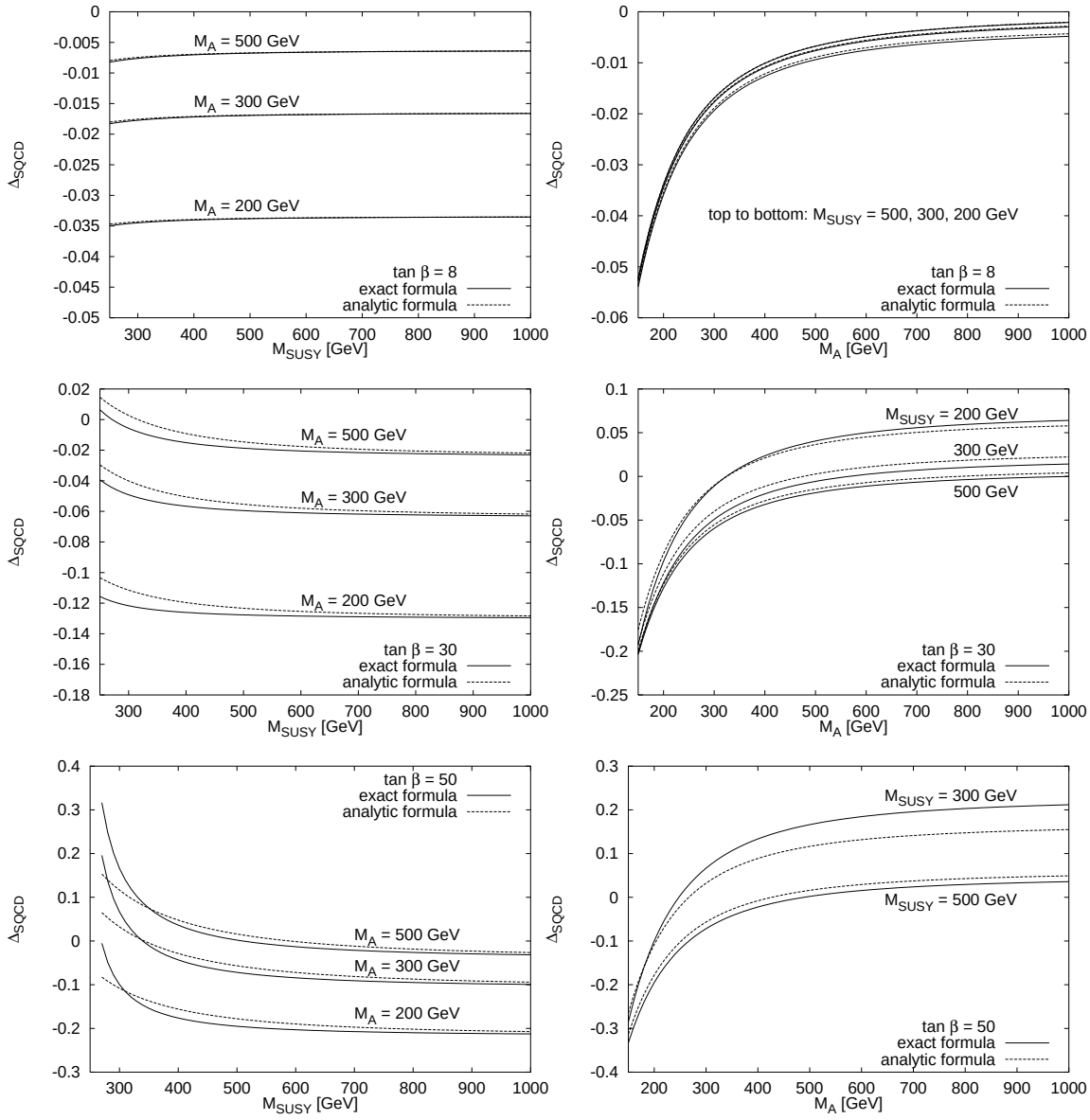

Figure 3: Δ_{SQCD} for $M_{SUSY} = M_L = M_R = M_S = M_{\tilde{g}} = \mu = A_b$, with $\tan\beta = 8$ (top panels), 30 (middle panels), and 50 (bottom panels). The solid lines are based on the exact one-loop formula and the dashed lines are based on the analytic approximation of eq. 4.5. In the left-hand panels we plot Δ_{SQCD} as a function of M_{SUSY} for $M_A = 200$, 300, and 500 GeV. In the right-hand panels we plot Δ_{SQCD} as a function of M_A for $M_{SUSY} = 200$, 300, and 500 GeV. For $\tan\beta = 50$, the value of $M_{SUSY} = 200$ GeV yields a negative mass-squared for the lighter sbottom, so this value is not shown in the bottom right panel.

tends to a non-vanishing constant, and this constant tends to zero in the large M_{SUSY} limit.

Notice that from the numerical comparison between the exact and analytic formulae in fig. 3, we can conclude that our expansion is a good approximation for large enough SUSY mass parameters. In particular, it is reasonably accurate for M_{SUSY} larger than 300 GeV. Also, it is clear that as $\tan\beta$ grows, not only does Δ_{SQCD} increase in magnitude, but the agreement between the exact and analytic formulae becomes worse at low M_{SUSY}. This is due to the fact that the splitting between the squared masses of the two sbottoms in the maximal mixing case is proportional to $m_b \tan\beta$, which we have taken to be of order M_{EW} in our expansion. As $\tan\beta$ increases, the mass of the lighter sbottom decreases, and the higher order terms that we have neglected in our expansion become more important.

All numerical results presented so far correspond to $\mu M_{\tilde{g}} > 0$. In the case of $\mu M_{\tilde{g}} < 0$, the qualitative features of $|\Delta_{SQCD}|$ remain unchanged. From the analytic formulae derived in this section, one can see that at large $\tan\beta$ the dominant effect of changing the sign of $\mu M_{\tilde{g}}$ is to change the overall sign of Δ_{SQCD}. We can illustrate this point in the simple limiting case in which all SUSY mass parameters and M_A are equal. Simplifying eq. 4.5 in this limit, we end up with a simple formula for the case of $\mu M_{\tilde{g}} > 0$:

$$\Delta_{SQCD} = \frac{\alpha_s}{3\pi}\left\{\frac{M_Z^2}{3M_{SUSY}^2}\cos 2\beta\,(7\tan\beta - 2) + \frac{M_{h^0}^2}{12M_{SUSY}^2}\,(\tan\beta - 1)\right.$$
$$\left. + \frac{m_b^2\tan^2\beta}{2M_{SUSY}^2}\,(\tan\beta - 4) + \mathcal{O}\left(\frac{m_b M_{EW}}{M_{SUSY}^2}\right)\right\}, \qquad (4.12)$$

where $M_{SUSY} = M_S = M_{\tilde{g}} = \mu = A_b = M_A$. To obtain the result for $\mu M_{\tilde{g}} < 0$, one replaces $\tan\beta$ with $-\tan\beta$ in eq. 4.12. The formula of eq. 4.12 is plotted in fig. 4 for three values of $\tan\beta$ and both signs of μ (taking $M_{\tilde{g}}$ to be positive, by convention). Clearly, Δ_{SQCD} decouples like (M_{EW}^2/M_{SUSY}^2), but this decoupling is delayed at large $\tan\beta$. For example, even at $M_{SUSY} =$ 1 TeV, $|\Delta_{SQCD}| \simeq 1\%$ for $\tan\beta \sim 30$. Note that as expected, changing the sign of μ simply changes the sign of the dominant contribution to Δ_{SQCD}. In the remainder of our analysis, we will display results only for $\mu > 0$.

Next, we consider the decoupling of the SQCD corrections to the $h^0 b\bar{b}$ coupling as individual SUSY particles become heavy compared to the common SUSY mass scale. We examine three cases: large M_S with maximal sbottom mixing, large $M_{\tilde{g}}$ with maximal sbottom mixing, and one heavy sbottom state with near-zero sbottom mixing.

We first consider the case of large M_S with maximal sbottom mixing, with $M_S \gg M_{\tilde{g}} \sim \mu \sim A_b \gg M_{EW}$. If M_S is taken large while the rest of the SUSY mass parameters remain fixed, then we may expand the functions

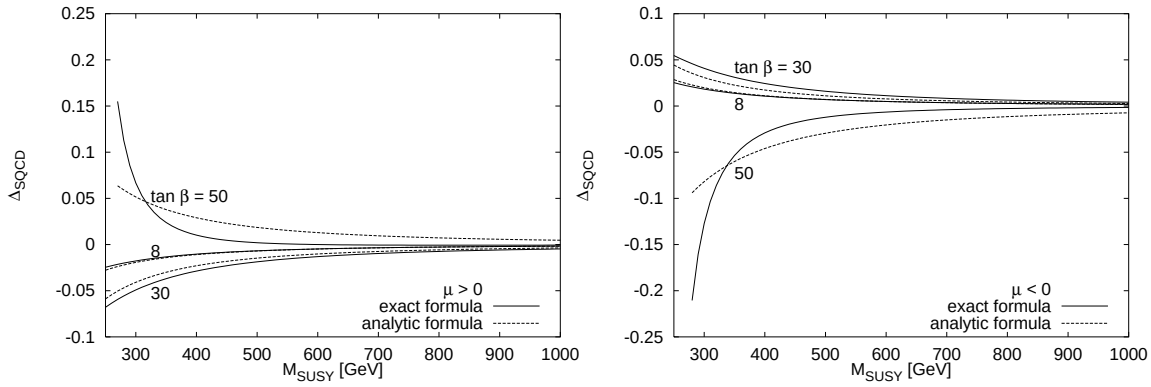

Figure 4: $\Delta_{\rm SQCD}$ as a function of M_{SUSY} for $M_{SUSY} = M_L = M_R = M_S = M_{\tilde{g}} = |\mu| = A_b = M_A$ and $\tan\beta = 8$, 30, 50. Both positive and negative μ cases are shown. The solid lines are based on the exact one-loop formula and the dashed lines are based on the analytic approximation of eq. 4.12.

$f_i(R)$ in eq. 4.5 for $M_S \gg M_{\tilde{g}}$, or $R \ll 1$. The result is:

$$\Delta_{SQCD} = \frac{\alpha_s}{3\pi}\left\{\frac{-2\mu M_{\tilde{g}}}{M_S^2}(\tan\beta + \cot\alpha) + \frac{M_Z^2}{M_S^2}\frac{\cos\beta\sin(\alpha+\beta)}{\sin\alpha}I_3^b + \mathcal{O}\left(\frac{M^4}{M_S^4}\right)\right\}, \tag{4.13}$$

where M is one of the lighter SUSY particle masses. Note that in this limit, the SQCD corrections decouple like M^2/M_S^2 even for light M_A. Thus it is only in the case of large $M_{\tilde{g}}$ and μ, of the same order as M_S, that large M_A is required for decoupling. In fig. 5 we plot the exact one-loop expression for Δ_{SQCD} and the expansions of eqs. 4.5 and 4.13 as a function of M_S, for fixed $M_{\tilde{g}} = \mu = A_b = M_A = 200$ GeV and three different values of $\tan\beta$. This figure shows the decoupling of Δ_{SQCD} with M_S as discussed above.

Similarly we examine the case of a very heavy gluino compared to the rest of the SUSY spectrum. We still focus on the case of maximal sbottom mixing. Expanding the functions $f_i(R)$ in eq. 4.5 for $M_{\tilde{g}} \gg M_S$, or $R \gg 1$, we see that in this case the SQCD corrections decouple with the gluino mass like $M/M_{\tilde{g}}$, where again M is one of the other light SUSY masses:

$$\Delta_{SQCD} = \frac{\alpha_s}{3\pi}\left\{\frac{2\mu}{M_{\tilde{g}}}(\tan\beta + \cot\alpha)\left[1 - \log\left(\frac{M_{\tilde{g}}^2}{M_S^2}\right)\right] - \frac{Y_b}{3M_{\tilde{g}}}\frac{M_{h^0}^2}{M_S^2}\right. \tag{4.14}$$
$$\left. + \frac{2X_b}{M_{\tilde{g}}}\frac{M_Z^2}{M_S^2}\frac{\cos\beta\sin(\alpha+\beta)}{\sin\alpha}I_3^b - \frac{\mu^2 m_b^2\tan^2\beta}{M_{\tilde{g}}M_S^4}\left(Y_b - 2A_b\frac{\cot\alpha}{\tan\beta}\right) + \mathcal{O}\left(\frac{M^2}{M_{\tilde{g}}^2}\right)\right\}.$$

Note that the decoupling of the SQCD corrections at large $M_{\tilde{g}}$ (with all other SUSY mass parameters held fixed) is very slow: Δ_{SQCD} falls off only as one power of $M_{\tilde{g}}$. This is due to the factor of $M_{\tilde{g}}$ in the numerator of eqs. 3.6 and 3.8, which arises from the gluino propagator. Δ_{SQCD} is also enhanced by the

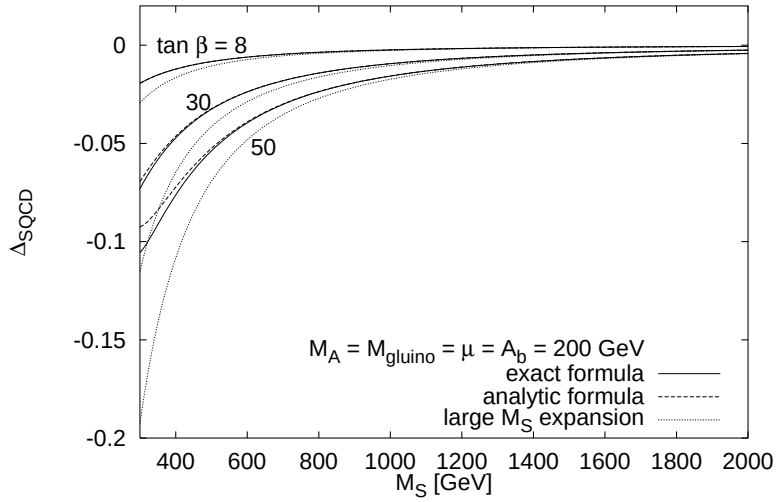

Figure 5: $\Delta_{\rm SQCD}$ as a function of M_S (assuming $M_L = M_R = M_S$) for $M_{\tilde{g}} = \mu = A_b = M_A = 200$ GeV and $\tan\beta = 8, 30, 50$ (top to bottom). Solid lines are based on the exact one-loop expression, dashed lines are based on the analytic expansion of eq. 4.5, and dotted lines are based on the large M_S expansion of eq. 4.13.

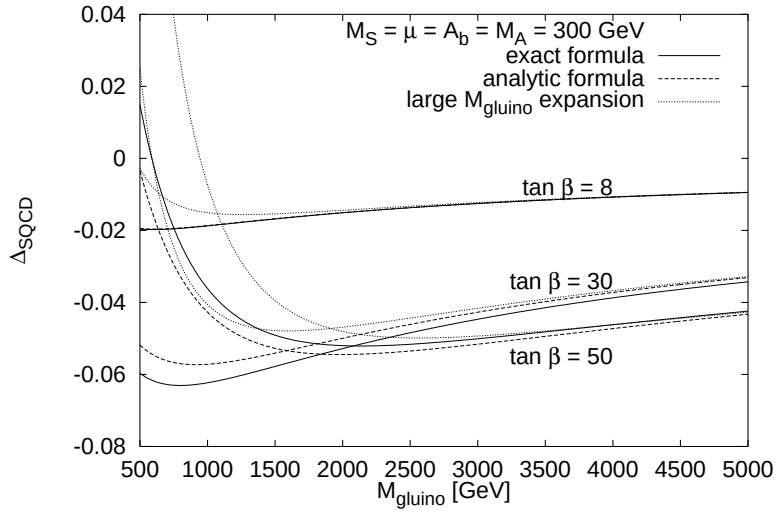

Figure 6: $\Delta_{\rm SQCD}$ as a function of $M_{\tilde{g}}$ for $M_L = M_R = M_S = \mu = A_b = M_A =$ 300 GeV and $\tan\beta = 8, 30, 50$. Solid lines are based on the exact one-loop expression, dashed lines based on are the analytic expansion of eq. 4.5, and dotted lines are based on the expansion for large $M_{\tilde{g}}$ of eq. 4.14.

factor $\log(M_{\tilde{g}}^2/M_S^2)$. We again see the phenomenon of delayed decoupling at large $\tan\beta$ due to the terms in eq. 4.14 proportional to either X_b or Y_b.

In fig. 6 we plot the exact one-loop expression for Δ_{SQCD} and the expansions of eqs. 4.5 and 4.14 as a function of $M_{\tilde{g}}$, for $M_S = \mu = A_b = M_A = 300$ GeV and three different values of $\tan\beta$. This figure shows the slow decoupling of Δ_{SQCD} with $M_{\tilde{g}}$. For example, for $M_{\tilde{g}} = 500$ GeV and $\tan\beta = 30$, $\Delta_{SQCD} \simeq -6\%$ for $M_S = \mu = A_b = M_A = 300$ GeV. If the latter masses are reduced to 200 GeV, one finds $\Delta_{SQCD} \simeq -13\%$, which is a significant correction. Fig. 6 also illustrates the validity of the large gluino mass expansion. This expansion is particularly poor for large values of $\tan\beta$ out to a very large gluino mass of about 2000 GeV.

Finally we study the case in which one of the sbottoms becomes heavy while the other sbottom mass and the rest of the SUSY mass parameters are fixed. We choose $M_R \gg M_L \sim M_{\tilde{g}} \sim \mu \sim A_b \gg M_{EW}$, so that $M_{\tilde{b}_2} \gg M_{\tilde{b}_1}$. This is necessarily the case of near-zero sbottom mixing. Expanding eq. 4.7 in inverse powers of $M_{\tilde{b}_2}$, we find:

$$\begin{aligned}\Delta_{SQCD} = \frac{\alpha_s}{3\pi}\Bigg\{ & \frac{2}{3}\frac{M_Z^2}{M_{\tilde{b}_1}^2}\frac{\cos\beta\sin(\alpha+\beta)}{\sin\alpha}(I_3^b - Q_b s_W^2) f_5(R_1) \\ & + \frac{2\mu M_{\tilde{g}}}{M_{\tilde{b}_2}^2}(\tan\beta + \cot\alpha)\left[h(R_1) + \log\left(\frac{M_{\tilde{g}}^2}{M_{\tilde{b}_2}^2}\right)\right] \\ & + \frac{M_Z^2}{M_{\tilde{b}_2}^2}\frac{\cos\beta\sin(\alpha+\beta)}{\sin\alpha}\left[(I_3^b - Q_b s_W^2)\frac{2M_{\tilde{g}}X_b}{M_{\tilde{b}_1}^2} f_1(R_1) + Q_b s_W^2\right] \\ & + \frac{2}{3}\frac{\mu^2 m_b^2 \tan\beta\cot\alpha}{M_{\tilde{b}_1}^2 M_{\tilde{b}_2}^2} f_5(R_1) + \mathcal{O}\left(\frac{M^4}{M_{\tilde{b}_2}^4}\right)\Bigg\}\,, \end{aligned} \tag{4.15}$$

where again M is one of the other light SUSY masses and the function $h(R_1)$ is given in the Appendix. Note that the first term does *not* decouple as $M_{\tilde{b}_2}$ is taken large. This behavior is independent of the value of M_A (and therefore holds even if $M_A \to \infty$). However, this first term is not enhanced by large $\tan\beta$ and is numerically negligible as can be seen in fig. 7. The terms that are enhanced by large $\tan\beta$ decouple like $M^2/M_{\tilde{b}_2}^2$. In fig. 7 we plot the exact one-loop expression for Δ_{SQCD} and the expansions of eqs. 4.7 and 4.15, as a function of $M_{\tilde{b}_2}$, for $M_{\tilde{b}_1} = M_{\tilde{g}} = \mu = A_b = M_A = 200$ GeV and three different values of $\tan\beta$. Clearly, in order for $\Delta_{\rm SQCD}$ to be large in the case of near-zero sbottom mixing, both of the sbottoms must be reasonably light. Note however that, due to the enhancement in $\tan\beta$, the $1/M_{\tilde{b}_2}^2$ suppression is not so small. As an example, for $\tan\beta = 50$, $M_{\tilde{b}_1} = M_{\tilde{g}} = \mu = A_b = M_A = 200$ GeV and $M_{\tilde{b}_2} = 500$ GeV [1000 GeV], one obtains $\Delta_{\rm SQCD} \simeq -10\%$ [-5%].

The various cases examined in this section can be summarized by specifying the behavior of C_1 and C_2 of eq. 4.11 on the model parameters. In Table 1, four cases are shown. In all cases, M_{SUSY} is identified with the

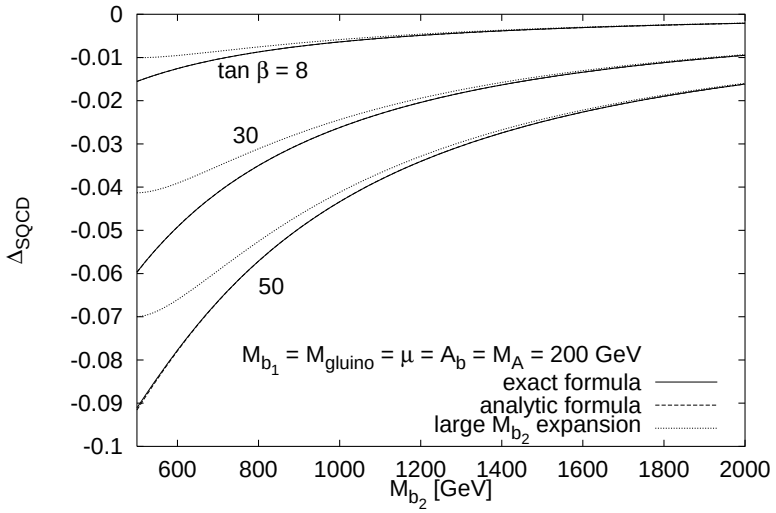

Figure 7: $\Delta_{\rm SQCD}$ as a function of $M_{\tilde{b}_2}$, with $M_{\tilde{b}_1} = M_{\tilde{g}} = \mu = A_b = M_A =$ 200 GeV and $\tan\beta = 8, 30, 50$. Solid lines are based on the exact one-loop formula, dashed lines based on are the analytic expansion for near-zero sbottom mixing of eq. 4.7, and dotted lines are based on the expansion for large $M_{\tilde{b}_2}$ of eq. 4.15.

largest supersymmetry-breaking mass, while M refers to a possible intermediate supersymmetric mass scale (with $M_{EW} \ll M \ll M_{SUSY}$). The presence of a factor of $\tan\beta$ (unless multiplied by M/M_{SUSY}) indicates delayed decoupling. In the case of $M_{\tilde{g}} = M_{SUSY}$, $C_2 \sim (M_{SUSY}/M)\tan\beta$ implies a delayed decoupling that vanishes only as a single power of $1/M_{SUSY}$. Finally, in the case of large $M_{\tilde{b}_2}$, $C_2 \sim M_{SUSY}^2/M^2$ implies no decoupling as $M_{SUSY} \to \infty$ with M held fixed. This is not a violation of the usual decoupling theorem [2,3], since in the latter case, only part of the supersymmetric spectrum has been removed from the low-energy effective theory. Decoupling is recovered in the limit of $M \to \infty$, as expected.

Case	$\widetilde{b}$ mixing	C_1	C_2
$M_S \simeq M_{\tilde{g}} = M_{SUSY}$	maximal	$\tan\beta$	$\tan\beta$
$M_S = M_{SUSY} \gg M$	maximal	$(M^2/M_{SUSY}^2)\tan\beta$	1
$M_{\tilde{g}} = M_{SUSY} \gg M$	maximal	$(M/M_{SUSY})\tan\beta$	$(M_{SUSY}/M)\tan\beta$
$M_{\tilde{b}_2} = M_{SUSY} \gg M$	near-zero	$(M^2/M_{SUSY}^2)\tan\beta$	M_{SUSY}^2/M^2

Table 1: Approach to decoupling of the one-loop $\mathcal{O}(\alpha_s)$ radiative corrections to the $h^0 b\bar{b}$ vertex: $\Delta_{SQCD} \sim C_1(M_{EW}^2/M_A^2) + C_2(M_{EW}^2/M_{SUSY}^2)$. See text for further discussion.

5 Conclusions

In this paper we have studied the one loop SQCD corrections to the $h^0 b\bar{b}$ coupling in the limit of large SUSY masses. In order to understand analytically the behavior of the corrections in this limit, we have performed expansions for the SUSY mass parameters large compared to the electroweak scale. We have shown that for the SUSY mass parameters and M_A large and all of the same order, the SQCD corrections decouple like the inverse square of these mass parameters. However, if the mass parameters are not all of the same size, then this behavior can be modified. If M_A is light, then the SQCD corrections to the $h^0 b\bar{b}$ coupling generically do not decouple in the limit of large SUSY mass parameters. In this case, the low-energy theory at the electroweak scale contains two full Higgs doublets with Higgs-fermion couplings of the general type-III model.

We have also examined three cases in which there is a hierarchy among the SUSY mass parameters. In the case of maximal sbottom mixing with M_S large and the other SUSY mass parameters and M_A of order a common mass scale M (chosen such that $M_{EW} \ll M \ll M_S$), the SQCD corrections decouple like M^2/M_S^2. Second, we examined the case of a large gluino mass with the other SUSY mass parameters of order a common mass scale M (chosen such that $M_{EW} \ll M \ll M_{\tilde{g}}$). In this case we found that the SQCD corrections decouple more slowly, like $(M/M_{\tilde{g}}) \log(M_{\tilde{g}}^2/M_S^2)$. Finally, we examined the case in which one sbottom is much heavier than the other SUSY mass parameters, which are fixed at a scale M. In this case the mixing angle in the sbottom sector is near zero. We found that the piece of the SQCD corrections that is enhanced at large $\tan\beta$ decouples like $M^2/M_{\tilde{b}_2}^2$. There is also a piece of the SQCD corrections that does not decouple as $M_{\tilde{b}_2}$ is taken large, but it is not enhanced by $\tan\beta$ and is numerically negligible compared to the decoupling piece, up to a very high value of the heavier sbottom mass.

The decoupling behavior of the SQCD corrections to the $h^0 b\bar{b}$ coupling implies that distinguishing the lightest MSSM Higgs boson from the SM Higgs boson will be very difficult if A^0 and the SUSY spectrum are heavy, even after one-loop SUSY corrections are taken into account. However, because of the enhancement at large $\tan\beta$, the onset of decoupling is delayed, and the corrections can still be at the percent level for $\tan\beta \sim 50$ and all SUSY mass parameters and M_A of order 1 TeV. If one or both of the sbottoms, the gluino, and/or A^0 lie below the TeV scale, then the SQCD corrections will be larger still. The decoupling limit provides a challenge for Higgs searches at future colliders. Even if the light CP-even Higgs boson is found, the direct discovery of supersymmetric particles may be essential for unraveling the origin of electroweak symmetry breaking.

Acknowledgments

We wish to thank M. Carena, K. Matchev, C. E. M. Wagner and G. Weiglein for interesting discussions. M.H., S.P., S.R. and D.T. kindly thank T. Hahn for providing the code of LoopTools (which was used in the calculation) and for many helpful suggestions. H.L. is grateful to G. Kribs for a discussion on models of SUSY breaking.

This work has been supported in part by the Spanish Ministerio de Educacion y Cultura under project CICYT AEN97-1678. S.R. has been partially supported by the European Union through contract ERBFMBICT972474. H.E.H. is supported in part by the U.S. Department of Energy under contract DE-FG03-92ER40689. Fermilab is operated by Universities Research Association Inc. under contract no. DE-AC02-76CH03000 with the U.S. Department of Energy.

Appendix

A Expansions of loop functions

In this Appendix we define our notation for the two- and three-point integrals that appear in eqs. 3.6 and 3.8 and give formulae for their expansions in powers of the SUSY mass parameters.

We follow the definitions and conventions of [34]. The two-point integrals are given by:

$$\mu^{4-D}\int\frac{d^Dk}{(2\pi)^D}\frac{\{1;k^\mu\}}{[k^2-m_1^2][(k+q)^2-m_2^2]}=\frac{i}{16\pi^2}\left\{B_0;q^\mu B_1\right\}(q^2;m_1^2,m_2^2)\,. \tag{A.1}$$

The derivatives of the two-point functions are defined as follows:

$$B'_{0,1}(p^2;m_1^2,m_2^2)=\left.\frac{\partial}{\partial q^2}B_{0,1}(q^2;m_1^2,m_2^2)\right|_{q^2=p^2}\,. \tag{A.2}$$

Finally, the three-point integrals are given by:

$$\begin{aligned}\mu^{4-D}\int\frac{d^Dk}{(2\pi)^D}&\frac{\{1;k^\mu\}}{[k^2-m_1^2][(k+p_1)^2-m_2^2][(k+p_1+p_2)^2-m_3^2]}\\&=\frac{i}{16\pi^2}\left\{C_0;p_1^\mu C_{11}+p_2^\mu C_{12}\right\}(p_1^2,p_2^2,p^2;m_1^2,m_2^2,m_3^2)\,,\end{aligned} \tag{A.3}$$

where $p=-p_1-p_2$.

We now give the large M_{SUSY} expansions of the loop integrals.

A.1 Maximal $\tilde{b}_L - \tilde{b}_R$ mixing

The loop integrals are expanded as follows, where M_S^2 and Δ^2 are defined in eq. 4.3.

$$
\begin{aligned}
&C_0(m_b^2, M_{h^0}^2, m_b^2; M_{\tilde{g}}^2, M_{\tilde{b}_1}^2, M_{\tilde{b}_1}^2) \\
&\qquad \simeq -\frac{1}{2M_S^2} f_1(R) + \frac{\Delta^2}{3M_S^4} f_2(R) - \frac{\Delta^4}{4M_S^6} f_3(R) - \frac{M_{h^0}^2}{24M_S^4} f_4(R) \\
&C_0(m_b^2, M_{h^0}^2, m_b^2; M_{\tilde{g}}^2, M_{\tilde{b}_2}^2, M_{\tilde{b}_2}^2) \\
&\qquad \simeq -\frac{1}{2M_S^2} f_1(R) - \frac{\Delta^2}{3M_S^4} f_2(R) - \frac{\Delta^4}{4M_S^6} f_3(R) - \frac{M_{h^0}^2}{24M_S^4} f_4(R) \\
&C_0(m_b^2, M_{h^0}^2, m_b^2; M_{\tilde{g}}^2, M_{\tilde{b}_1}^2, M_{\tilde{b}_2}^2) \\
&\qquad \simeq -\frac{1}{2M_S^2} f_1(R) - \frac{\Delta^4}{12M_S^6} f_3(R) - \frac{M_{h^0}^2}{24M_S^4} f_4(R) \\
&C_{11}(m_b^2, M_{h^0}^2, m_b^2; M_{\tilde{g}}^2, M_{\tilde{b}_1}^2, M_{\tilde{b}_1}^2) \\
&\qquad \simeq \frac{1}{3M_S^2} f_5(R) - \frac{\Delta^2}{4M_S^4} f_4(R) + \frac{\Delta^4}{5M_S^6} f_6(R) + \frac{M_{h^0}^2}{30M_S^4} f_7(R) \\
&C_{11}(m_b^2, M_{h^0}^2, m_b^2; M_{\tilde{g}}^2, M_{\tilde{b}_2}^2, M_{\tilde{b}_2}^2) \\
&\qquad \simeq \frac{1}{3M_S^2} f_5(R) + \frac{\Delta^2}{4M_S^4} f_4(R) + \frac{\Delta^4}{5M_S^6} f_6(R) + \frac{M_{h^0}^2}{30M_S^4} f_7(R) \\
&B_0(m_b^2; M_{\tilde{g}}^2, M_{\tilde{b}_1}^2) - B_0(m_b^2; M_{\tilde{g}}^2, M_{\tilde{b}_2}^2) \simeq -\frac{\Delta^2}{M_S^2} f_1(R) \\
&B_0'(m_b^2; M_{\tilde{g}}^2, M_{\tilde{b}_1}^2) - B_0'(m_b^2; M_{\tilde{g}}^2, M_{\tilde{b}_2}^2) \simeq -\frac{\Delta^2}{6M_S^4} f_8(R) \\
&B_1'(m_b^2; M_{\tilde{g}}^2, M_{\tilde{b}_1}^2) + B_1'(m_b^2; M_{\tilde{g}}^2, M_{\tilde{b}_2}^2) \simeq -\frac{1}{6M_S^2} f_4(R) - \frac{\Delta^4}{15M_S^6} f_9(R). \quad \text{(A.4)}
\end{aligned}
$$

The functions $f_i(R)$ are given in terms of the ratio $R \equiv M_{\tilde{g}}/M_S$:

$$
\begin{aligned}
f_1(R) &= \frac{2}{(1-R^2)^2}\left[1 - R^2 + R^2 \log R^2\right] \\
f_2(R) &= \frac{3}{(1-R^2)^3}\left[1 - R^4 + 2R^2 \log R^2\right] \\
f_3(R) &= \frac{4}{(1-R^2)^4}\left[1 + \tfrac{3}{2}R^2 - 3R^4 + \tfrac{1}{2}R^6 + 3R^2 \log R^2\right] \\
f_4(R) &= \frac{4}{(1-R^2)^4}\left[\tfrac{1}{2} - 3R^2 + \tfrac{3}{2}R^4 + R^6 - 3R^4 \log R^2\right] \\
f_5(R) &= \frac{3}{(1-R^2)^3}\left[\tfrac{1}{2} - 2R^2 + \tfrac{3}{2}R^4 - R^4 \log R^2\right] \\
f_6(R) &= \frac{5}{(1-R^2)^5}\left[\tfrac{1}{2} - 4R^2 + 4R^6 - \tfrac{1}{2}R^8 - 6R^4 \log R^2\right] \\
f_7(R) &= \frac{5}{(1-R^2)^5}\left[\tfrac{1}{3} - 2R^2 + 6R^4 - \tfrac{10}{3}R^6 - R^8 + 4R^6 \log R^2\right]
\end{aligned}
$$

$$f_8(R) = \frac{12}{(1-R^2)^4}\left[\tfrac{1}{2} + 2R^2 - \tfrac{5}{2}R^4 + 2R^2\log R^2 + R^4\log R^2\right]$$
$$f_9(R) = \frac{5}{(1-R^2)^6}\Big[1 - 12R^2 - 36R^4 + 44R^6 + 3R^8 - 24R^6\log R^2 - 36R^4\log R^2\Big]\,. \qquad \text{(A.5)}$$

Note that in the special case $M_{\tilde{g}} = M_S$, $R = 1$ and $f_i(1) = 1$.

A.2 Near-zero $\tilde{b}_L - \tilde{b}_R$ mixing

The loop integrals are expanded as follows:

$$C_0(m_b^2, M_{h^0}^2, m_b^2; M_{\tilde{g}}^2, M_{\tilde{b}_1}^2, M_{\tilde{b}_1}^2) \simeq -\frac{1}{2M_{\tilde{b}_1}^2} f_1(R_1) - \frac{M_{h^0}^2}{24M_{\tilde{b}_1}^4} f_4(R_1)$$
$$C_0(m_b^2, M_{h^0}^2, m_b^2; M_{\tilde{g}}^2, M_{\tilde{b}_2}^2, M_{\tilde{b}_2}^2) \simeq -\frac{1}{2M_{\tilde{b}_2}^2} f_1(R_2) - \frac{M_{h^0}^2}{24M_{\tilde{b}_2}^4} f_4(R_2)$$
$$C_0(m_b^2, M_{h^0}^2, m_b^2; M_{\tilde{g}}^2, M_{\tilde{b}_1}^2, M_{\tilde{b}_2}^2) \simeq -\frac{h_1(R_1,R_2)}{(M_{\tilde{b}_1}^2 - M_{\tilde{b}_2}^2)} + \frac{M_{h^0}^2\, h_2(R_1,R_2)}{(M_{\tilde{b}_1}^2 - M_{\tilde{b}_2}^2)^2}$$
$$C_{11}(m_b^2, M_{h^0}^2, m_b^2; M_{\tilde{g}}^2, M_{\tilde{b}_1}^2, M_{\tilde{b}_1}^2) \simeq \frac{1}{3M_{\tilde{b}_1}^2} f_5(R_1) + \frac{M_{h^0}^2}{30M_{\tilde{b}_1}^4} f_7(R_1)$$
$$C_{11}(m_b^2, M_{h^0}^2, m_b^2; M_{\tilde{g}}^2, M_{\tilde{b}_2}^2, M_{\tilde{b}_2}^2) \simeq \frac{1}{3M_{\tilde{b}_2}^2} f_5(R_2) + \frac{M_{h^0}^2}{30M_{\tilde{b}_2}^4} f_7(R_1)$$
$$B_0(m_b^2; M_{\tilde{g}}^2, M_{\tilde{b}_1}^2) - B_0(m_b^2; M_{\tilde{g}}^2, M_{\tilde{b}_2}^2) \simeq -h_1(R_1,R_2)$$
$$B_0'(m_b^2; M_{\tilde{g}}^2, M_{\tilde{b}_1}^2) - B_0'(m_b^2; M_{\tilde{g}}^2, M_{\tilde{b}_2}^2) \simeq \frac{1}{6M_{\tilde{b}_1}^2} f_2(R_1) - \frac{1}{6M_{\tilde{b}_2}^2} f_2(R_2)$$
$$B_1'(m_b^2; M_{\tilde{g}}^2, M_{\tilde{b}_1}^2) + B_1'(m_b^2; M_{\tilde{g}}^2, M_{\tilde{b}_2}^2) \simeq -\frac{1}{12M_{\tilde{b}_1}^2} f_4(R_1) - \frac{1}{12M_{\tilde{b}_2}^2} f_4(R_2), \qquad \text{(A.6)}$$

where $R_i \equiv M_{\tilde{g}}/M_{\tilde{b}_i}$ $(i = 1, 2)$. The functions $f_i(R)$ were given in eq. A.5. The functions $h_1(R_1, R_2)$ and $h_2(R_1, R_2)$ are defined as follows:

$$h_1(R_1,R_2) = h(R_1) - h(R_2), \qquad \text{with} \qquad h(R) = -\frac{\log R^2}{1-R^2},$$
$$h_2(R_1,R_2) = 1 + \frac{R_1^2 + R_2^2 - 2R_1^2R_2^2}{2(1-R_1^2)(1-R_2^2)} - \frac{1}{2(R_1^2 - R_2^2)}\left[\frac{\log R_1^2}{(1-R_1^2)^2}(R_1^2 + R_2^2 - 2R_1^4) - \frac{\log R_2^2}{(1-R_2^2)^2}(R_1^2 + R_2^2 - 2R_2^4)\right]. \qquad \text{(A.7)}$$

The functions h and h_2 have the following properties:

$$\begin{aligned} h(1) &= 1, \\ h_2(R_1, R_2) &= h_2(R_2, R_1), \\ h_2(1, R_2) &= \frac{1}{(1-R_2^2)^2}\left[\tfrac{5}{4} - R_2^2 - \tfrac{1}{4}R_2^4 + \left(\tfrac{1}{2} + R_2^2\right)\log R_2^2\right] . \end{aligned} \tag{A.8}$$

References

[1] H. E. Haber and Y. Nir, Nucl. Phys. **B335**, 363 (1990); H. E. Haber, in Proceedings of the US–Polish Workshop, Warsaw, Poland, September 21–24, 1994, edited by P. Nath, T. Taylor, and S. Pokorski (World Scientific, Singapore, 1995) pp. 49–63.

[2] A. Dobado, M. J. Herrero and S. Peñaranda, Eur. Phys. J. **C7**, 313 (1999); Eur. Phys. J. **C12**, 673 (2000); hep-ph/0002134.

[3] T. Appelquist and J. Carazzone, Phys. Rev. **D11**, 2856 (1975).

[4] M. Carena, S. Mrenna and C. E. M. Wagner, Phys. Rev. **D60**, 075010 (1999).

[5] M. Carena, S. Mrenna and C. E. M. Wagner, hep-ph/9907422.

[6] D. Rainwater, D. Zeppenfeld and K. Hagiwara, Phys. Rev. **D59**, 014037 (1999); T. Plehn, D. Rainwater and D. Zeppenfeld, Phys. Rev. **D61**, 093005 (2000).

[7] F. Borzumati, G. R. Farrar, N. Polonsky and S. Thomas, Nucl. Phys. **B555**, 53 (1999).

[8] K.S. Babu and C. Kolda, Phys. Lett. **B451**, 77 (1999).

[9] A. Dabelstein, Nucl. Phys. **B456**, 25 (1995).

[10] J. A. Coarasa, R. A. Jiménez and J. Solà, Phys. Lett. **B389**, 312 (1996).

[11] L. J. Hall, R. Rattazzi and U. Sarid, Phys. Rev. **D50**, 7048 (1994); R. Hempfling, Phys. Rev. **D49**, 6168 (1994); M. Carena, M. Olechowski, S. Pokorski and C. E. M. Wagner, Nucl. Phys. **B426**, 269 (1994).

[12] D. M. Pierce, J. A. Bagger, K. Matchev and R.-J. Zhang, Nucl. Phys. **B491**, 3 (1997).

[13] S. Heinemeyer, W. Hollik and G. Weiglein, hep-ph/0003022.

[14] G.L. Kane, G.D. Kribs, S.P. Martin and J.D. Wells, Phys. Rev. **D53**, 213 (1996); H. Baer and J.D. Wells, Phys. Rev. **D57**, 4446 (1998).

[15] W. Loinaz and J.D. Wells, Phys. Lett. **B445**, 178 (1998).

[16] E. Braaten and J. P. Leveille, Phys. Rev. **D22**, 715 (1980); N. Sakai, Phys. Rev. **D22**, 2220 (1980); T. Inami and T. Kubota, Nucl. Phys. **B179**, 171 (1981).

[17] M. Carena, D. Garcia, U. Nierste and C. E. M. Wagner, Nucl. Phys. **B577**, 88 (2000).

[18] H. Eberl, K. Hidaka, S. Kraml, W. Majerotto and Y. Yamada, hep-ph/9912463.

[19] J. F. Gunion, H. E. Haber, G. Kane and S. Dawson, *The Higgs Hunter's Guide* (Addison–Wesley, Reading, MA, 1990) [errata: hep-ph/9302272].

[20] J. F. Gunion and H. E. Haber, Nucl. Phys. **B272**, 1 (1986); **B278**, 449 (1986) [E: **B402**, 567 (1993)].

[21] H. E. Haber and R. Hempfling, Phys. Rev. Lett. **66**, 1815 (1991); Phys. Rev. **D48**, 4280 (1993). Y. Okada, M. Yamaguchi and T. Yanagida, Prog. Theor. Phys. **85**, 1 (1991); Phys. Lett. **B262**, 54 (1991); J. Ellis, G. Ridolfi and F. Zwirner, Phys. Lett. **B257**, 83 (1991); Phys. Lett. **B262**, 477 (1991); R. Barbieri and M. Frigeni, Phys. Lett. **B258**, 167 (1991); Phys. Lett. **B258**, 395 (1991);

[22] R. Hempfling and A. H. Hoang, Phys. Lett. **B331**, 99 (1994); J. A. Casas, J. R. Espinosa, M. Quirós and A. Riotto, Nucl. Phys. **B436**, 3 (1995) [E: **B439**, 466 (1995)]; M. Carena, J. R. Espinosa, M. Quirós and C. E. M. Wagner, Phys. Lett. **B355**, 209 (1995); M. Carena, M. Quirós and C. E. M. Wagner, Nucl. Phys. **B461**, 407 (1996); H. E. Haber, R. Hempfling and A. H. Hoang, Z. Phys. **C75**, 539 (1997).

[23] J. R. Espinosa and R.-J. Zhang, JHEP **0003**, 026 (2000); hep-ph/0003246.

[24] P. H. Chankowski, S. Pokorski and J. Rosiek, Phys. Lett. **B274**, 191 (1992); Nucl. Phys. **B423**, 437 (1994); A. Dabelstein, Z. Phys. **C67**, 495 (1995).

[25] S. Heinemeyer, W. Hollik and G. Weiglein, Phys. Rev. **D58**, 091701 (1998); Phys. Lett. **B440**, 296 (1998); Eur. Phys. J. **C9**, 343 (1999); Phys. Lett. **B455**, 179 (1999).

[26] M. Carena, H. E. Haber, S. Heinemeyer, W. Hollik, C. E. M. Wagner and G. Weiglein, Nucl. Phys. **B580**, 29 (2000).

[27] P. Bock *et al.* [ALEPH, DELPHI, L3 and OPAL Collaborations and the LEP working group for Higgs boson searches], CERN-EP-2000-055 (April, 2000).

[28] T. Affolder *et al.* [CDF Collaboration], Phys. Rev. Lett. **84**, 5704 (2000).

[29] The ALEPH Collaboration, ALEPH 2000-012 CONF 2000-009, submitted to the 2000 Winter Conferences.

[30] S. Abachi *et al.* [D0 Collaboration], Phys. Rev. Lett. **75**, 618 (1995); F. Abe *et al.* [CDF Collaboration], Phys. Rev. **D56**, R1357 (1997).

[31] D. Atwood, L. Reina and A. Soni, Phys. Rev. **D55**, 3156 (1997) and references therein.

[32] L. Randall and R. Sundrum, Nucl. Phys. **B557**, 79 (1999); G. F. Giudice, M. A. Luty, H. Murayama, and R. Rattazzi, JHEP **9812**, 027 (1998).

[33] G. D. Kribs, Phys. Rev. **D62**, 015008 (2000).

[34] W. Hollik, in *Precision Tests of the Standard Electroweak Model*, edited by P. Langacker (World Scientific, Singapore, 1995), p. 37–116.